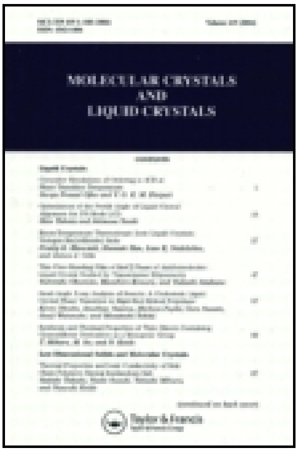

Molecular Crystals and Liquid Crystals
Publication details, including instructions for authors and subscription information:
http://www.tandfonline.com/loi/gmcl20

All-Optical Liquid Crystal Waveguide on Silicon

M. Trotta [a], R. Asquini [a], A. d'Alessandro [a] & R. Beccherelli [b]

[a] Department of Information Engineering, Electronics and Telecommunications, Sapienza University of Rome, Via Eudossiana, 18 00184 Rome - Italy

[b] Consiglio Nazionale delle Ricerche - Istituto per la Microelettronica e Microsistemi Via del Fosso del Cavaliere, 100 - 00133, Rome - Italy

Version of record first published: 07 Oct 2011

To cite this article: M. Trotta, R. Asquini, A. d'Alessandro & R. Beccherelli (2011): All-Optical Liquid Crystal Waveguide on Silicon, Molecular Crystals and Liquid Crystals, 549:1, 100-105

To link to this article: http://dx.doi.org/10.1080/15421406.2011.581153

Mol. Cryst. Liq. Cryst., Vol. 549: pp. 100–105, 2011

ISSN: 1542-1406 print/1563-5287 online
DOI: 10.1080/15421406.2011.581153

All-Optical Liquid Crystal Waveguide on Silicon

M. TROTTA,[1,*] R. ASQUINI,[1] A. D'ALESSANDRO,[1]
AND R. BECCHERELLI[2]

[1]Department of Information Engineering, Electronics and Telecommunications, Sapienza University of Rome, Via Eudossiana, 18 00184 Rome – Italy
[2]Consiglio Nazionale delle Ricerche – Istituto per la Microelettronica e Microsistemi Via del Fosso del Cavaliere, 100 - 00133 Rome - Italy

In this paper we demonstrate nonlinear optical properties of a channel waveguide made of E7 nematic liquid crystal infiltrated in a SiO_2/Si V-groove. Light in C-Band (1530-1565 nm), fiber coupled to the core of the liquid crystal waveguide, was optically modulated by the optical beam itself, with a power below 25 mW. A bias voltage was applied to induce a liquid crystal orientation over the Freedericksz threshold and a further director reorientation was obtained by increasing the optical beam. The effect of optical modulation for different applied voltages obtained experimentally was modelled including both opto and electro-optical effects.

Keywords All-optical waveguides; liquid crystals; electro-optic effect; silicon photonics; nonlinear optics

Introduction

All-optical photonic components can exploit more efficiently the huge band of the optical fibers and bring a lot of advantages, such as bit rate independency, flexibility, scalability to many applications [1–5]. The employment of all-optical devices can be also important for the development of research in the field of optical sensing, image processing and optical computing [6, 7]. In recent years, all-optical components have attracted increasing attention as a mean to exert control on micro-optofluidics systems [8, 9]. The operation principle of all-optical components is related to the nonlinearity of materials used to realize the devices. In this context, the research is focused on new materials with high nonlinear optical effects, which require low power optical control.

Liquid crystals (LC) are highly optically nonlinear materials whose physical properties are easily perturbed by an applied optical field [10]. They are characterized by large electro- and opto-optical reorientational responses, while exhibiting extended transparency from ultraviolet to mid infrared, low scattering losses, in addition to well developed chemistry, physics and technology. In this context, several electro-optic devices were proposed based on guiding properties of LC [11, 12], discrete spatial solitons [13] and all-optical switching [14]. Recently the LC properties have attracted a lot of interest in the innovative fields of biomedical and lab-on-chip applications [15, 16].

In this paper, we report on the experimental and theoretical demonstration of self-modulation of a light beam in the C-Band confined in a LC waveguide (LCW). The device is composed of a micromachined silicon V-groove filled with the nematic LC (NLC) E7.

*Corresponding author. E-mail: trotta@die.uniroma1.it

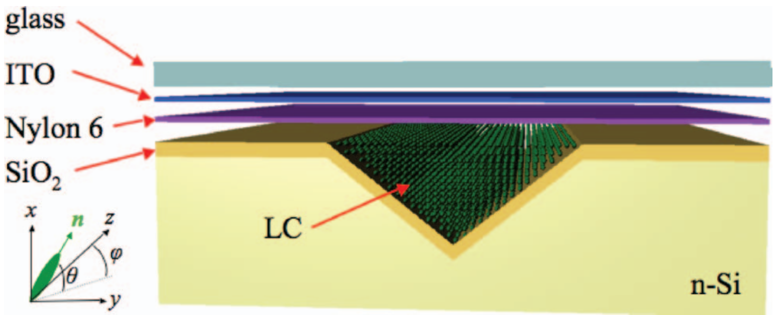

Figure 1. Schematic illustration of a LCW made of NLC embedded in a silica on silicon V-groove.

After reporting on the fabrication process, we present the experimental results of the self-modulation of the light beam propagating in the core of the waveguide. A model describing the nonlinear behaviour of the device is also presented showing good agreement with the experiment.

Device Structure and Fabrication

The optical waveguide structure schematically illustrated in Figure 1 is made of SiO_2/Si V-groove filled with the NLC E7. It consists of a core with a triangular cross-section with an upper width of 15 μm, a SiO_2 buffer layer and an ITO coated top glass cover. A Nylon 6 layer has been deposited and rubbed on the cover glass to provide uniaxial alignment of the liquid crystal. The structure and the fabrication process are described in details in previous works [12–14, 17]. A thin layer of Nylon 6 was rubbed after the deposition on the ITO electrode to promote the alignment of LC molecules along the propagation direction. The n-doped silicon substrate is used as counter electrode. NOA61 UV adhesive by Norland is used to seal the input and output and to define neat interfaces with NLC core of the waveguide [18]. Table 1 reports refractive indices of the materials, where $n_{//}$ and $n_{\perp}$ are the two indices of refraction parallel and perpendicular to the molecular axis of the NLC respectively.

Table 1. Refractive indices of the LCW materials

Material	Refractive index at $\lambda = 1550$ nm
LC E7	$n_{//} = 1.689$ $n_{\perp} = 1.502$
SiO_2	$n = 1.444$
n-Si	$n = 3.478$
D263 glass	$n = 1.516$
NOA61	$n = 1.542$

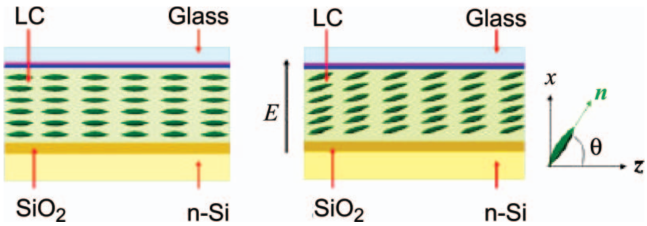

Figure 2. Schematic illustration of the device working principle without (left) and with (right) applied electric field.

Working Principle

The optical confinement of a laser beam at the wavelength of 1560 nm in a 15 μm wide LCW, butt-coupled by a single mode fiber [19], is achieved when the effective refractive index of the LCW is higher than the glass-SiO_2 cladding refractive index. When no electric field is applied on the LCW, the LC ordinary refractive index, corresponding to $n_\perp = 1.5$, is sensed by both TE and TM polarizations. Such refractive index at the wavelength of 1560 nm is lower than the one of the D263 cover glass and no light propagation occurs. While progressively increasing the electric field on the structure produced by an applied voltage or by the propagation beam itself, a molecular tilt reorientation occurs corresponding to an increase of the refractive index for TM input polarization (Figure 2). Guided propagation is enabled when the LC effective refractive index is higher than the glass refractive index.

Waveguide Modelling

The nonlinear behaviour of the LCW is modelled by considering both the electrically [20] and optically induced molecular reorientation. A bias applied voltage is used to induce a LC pretilt over the Freedericksz threshold. The LC director spatial reorientation is computed by minimizing the free energy density F reported in Equation (1), composed of the elastic $F_{elastic}$, electrostatic $F_{electrostatic}$ and optical $F_{optical}$ contribution [21]:

$$\begin{aligned} F &= F_{elastic} + F_{electrostatic} + F_{optical} \\ &= \frac{1}{2}(K_{11}(\nabla \cdot \boldsymbol{n})^2 + K_{22}(\boldsymbol{n} \cdot (\nabla \times \boldsymbol{n}))^2 + K_{33}(\boldsymbol{n} \times (\nabla \times \boldsymbol{n}))^2) \\ &\quad - \frac{1}{2}\varepsilon_0(\Delta\, \varepsilon_{es}(\boldsymbol{n} \cdot \boldsymbol{E_{es}})^2 + \varepsilon_{\perp es}\boldsymbol{E_{es}} \cdot \boldsymbol{E_{es}} + \Delta\varepsilon_{op}(\boldsymbol{n} \cdot \boldsymbol{E_{op}})^2 + \varepsilon_{\perp op}\boldsymbol{E_{op}} \cdot \boldsymbol{E_{op}}) \end{aligned} \quad (1)$$

The elastic energy, also known as Oseen–Frank, indicated as $F_{elastic}$, depends on K_{11}, K_{22} and K_{33} which are the elastic constants of the NLC (splay, twist and bend respectively). $F_{electrostatic}$ represents the energy contribution due to the electric field $\boldsymbol{E_{es}}$ of an applied voltage V, where $\varepsilon_{\perp es}$ is the dielectric permittivity when an electric field at low frequency is applied perpendicular to the director $\boldsymbol{n}$ and $\Delta\varepsilon_{es}$ is the relative dielectric anisotropy. The last contribution $F_{optical}$ indicates the energy due to the electric field referred to the optical excitation ($\boldsymbol{E_{op}}$), where $\varepsilon_{\perp op}$ and $\Delta\varepsilon_{op}$ refer to the optical frequencies.

After a bias tilt due to the applied voltage, a further director reorientation is obtained by increasing the input power of the laser beam. The electric field is the solution of the

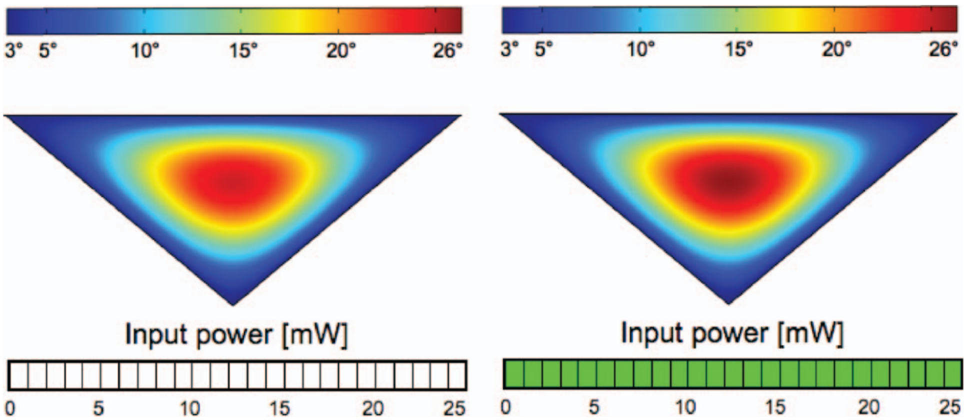

Figure 3. Contour maps of the molecular tilt distribution of the LCW with an applied bias of 2.17 V: without (left) and with (right) input optical power from a laser beam of 25 mW at a wavelength of 1560 nm.

Poisson equation solved using the finite element method applied to the anisotropic NLC. The minimization of F was achieved by solving the partial derivative Euler-Lagrange equation of F, implemented in the weak form by means of a finite element method. Strong anchoring was assumed with a pretilt of 3° at all boundaries for numerical stability. Lateral boundary condition and both LC tilt and twist angles were considered in the simulation. Calculations show that the azimuthal twist angle φ is perturbed by less than 5°, therefore its contribution to light propagation is negligible. The extraordinary refractive index of the NLC depends on the sum of the molecular tilt θ_V, induced by a low frequency electric field by means of an applied voltage, and the tilt θ_{op} induced by the optical electric field according to the Equation (2):

$$\boldsymbol{n}_e(\theta_V, \theta_{op}) = \frac{\boldsymbol{n}_\perp \boldsymbol{n}_{//}}{\sqrt{\boldsymbol{n}_\perp \,\mathbf{sin}^2(\theta_V + \theta_{op}) + \boldsymbol{n}_{//}\,\mathbf{cos}^2(\theta_V + \theta_{op})}} \tag{2}$$

The model describes the effect of optical field on the tilt angle as confirmed by the contour map of Figure 3, where the spatial distribution is modified when a laser beam of 25 mW at 1560 nm is applied for a bias voltage of 2.17 V.

Nonlinear Optical Characterization

In Figure 4 the set-up used to characterize the optical behaviour of the 15 μm LCW is presented. Single-mode optical fiber was butt-coupled both at the input and the output of the LCW connected to a DFB laser in the C-B. The polarization was controlled by a $\lambda/4 - \lambda/2 - \lambda/4$ wave plate sequence mounted on a fiber bench, so any state of polarization with negligible optical power loss can be obtained. To supply the bias voltage, the sample was driven by a symmetric +V/−V square wave of frequency 1 kHz.

The nonlinear optical behaviour can be observed by raising the optical power with TM polarization for a fixed applied voltage. Figure 5 shows a plot of the output optical power versus input power in solid line for two voltages bias at 6.7 V and 8 V. In the 6.7 V plot a nonlinear behaviour is observed when input optical power increases above 10 mW. The linear behaviour observed for 8 V bias is due to a saturation of the optical transmission

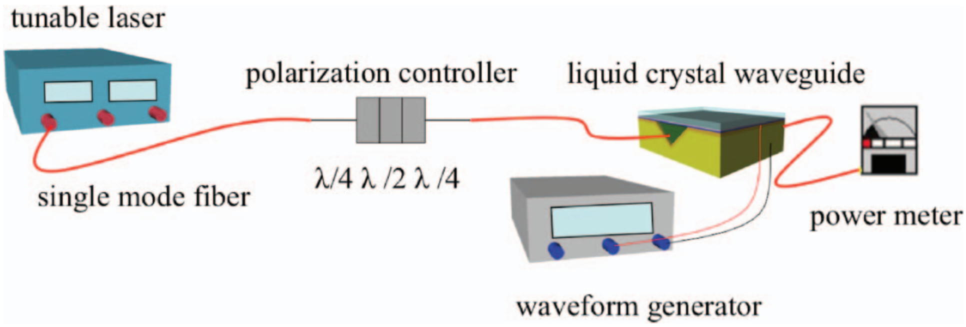

Figure 4. Measurement set-up used for nonlinear optical characterizations of LCW using fiber butt-coupling technique to collect the output signal measured by an optical power meter.

of the waveguide. The model can describe both nonlinear optical effect and transmission saturation. Figure 5 shows the experimental (solid line) and simulation (dashed line) results of the output optical power versus input power. In the 6.7 V plot a non linear behaviour is observed when input power increases above 10 mW. Theoretical curves at 2.17 V and 4 V follow the measured value for 6.7 V and 8 V respectively. In particular the model also includes optical losses for the corresponding voltage bias. The difference between the voltages of the theoretical curves and the experimental ones, are due in part to defects on the groove walls perturbing the LC orientation. Another contribution to such difference also comes from voltage drop along the electrodes, which smoothes out the square ac waveform and reduces the RMS voltage.

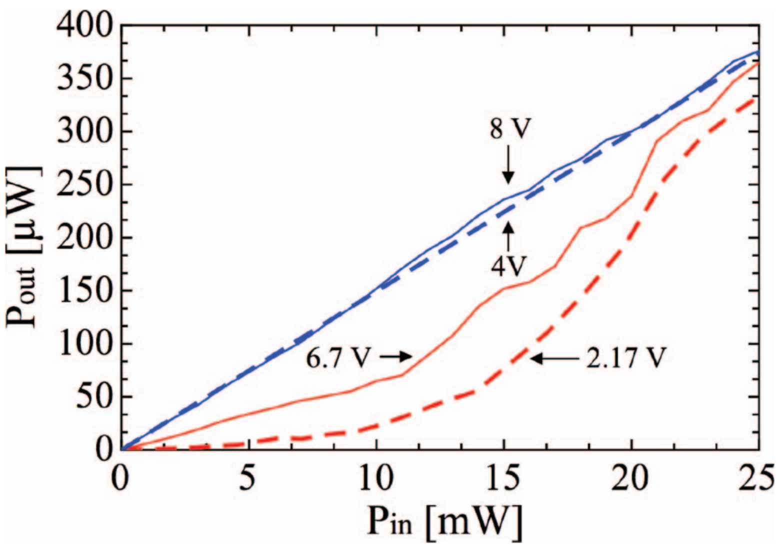

Figure 5. Plot of output power versus input power in which measurements for 6.7 V and 8 V applied voltage bias are compared with theoretical curves (dashed lines) at 2.17 V and 4 V.

Conclusion

A nonlinear optical LCW made of a commercial NLC mixture embedded in a SiO_2/Si is demonstrated both experimentally and theoretically. We modelled the nonlinear behaviour of the output power versus input power found experimentally by minimizing the total free energy, which includes the dielectric energy at optical frequencies. These preliminary results, far from their optimum performance, represent however a very encouraging demonstration of a first step towards truly working all-optical devices on silicon.

References

[1] A. A. M. Saleh and J. M. Simmons, *J. Lightw. Technol.* **24**(9), 3303–3321 (2006).
[2] I. P. Kaminow, *J. Lightw. Technol.* **26**(9), 994–1004 (2008).
[3] R. Nagarajan, et al., *IEEE J. Sel. Top. Quantum Electron.* **11**(1), 50–65 (2005).
[4] M. J. O'Mahony, C. Politi, D. Klonidis, R. Nejabati, and D. Simeonidou, *J. Lightw. Technol.* **24**(12), 4684–4696 (2006).
[5] J. Berthold, A. A. M. Saleh, L. Blair, and J. M. Simmons, *J. Lightw. Technol.* **26**(9), 1104–1118 (2008).
[6] D. A. B. Miller, *IEEE J. Select. Topics Quantum Electron.* **6**(6), 1312–1317 (2000).
[7] D. Huang, T. Sze, A. Landin, R. Lytel, and H. L. Davidson, *IEEE J. Sel. Topics Quantum Electron.* **9**(2), 614–623 (2003).
[8] C. Monat, P. Domachuk, and B. J. Eggleton, *Nat. Photonics* **1**, 106–114 (2007).
[9] D. Psaltis, S. R. Quake, and C. H. Yang, *Nature* **442**, 381–386 (2006).
[10] I.C. Khoo, *Liquid Crystals*, 2nd Edition, Wiley, NY (2007).
[11] A. d'Alessandro, R. Asquini, M. Menichella, and C. Ciminelli, *Mol. Cryst. Liq. Cryst.* **372**, 352 (2001).
[12] D. Donisi, B. Bellini, R. Beccherelli, R. Asquini, G. Gilardi, M. Trotta, and A. d'Alessandro, *IEEE J. Quantum Electron*. **46**(5) 762–768 (2010).
[13] M. Peccianti, A. De Rossi. G. Assanto, A. De Luca, C. Umeton, and I.C. Khoo, *Appl. Phys. Lett.* **77**(1), 126859 (2000).
[14] A. Fratalocchi and G. Assanto, *Appl. Phys. Lett.* **86**, 051109 (2005).
[15] N. A. Mortensen, S. Xiao, and J. Pedersen, *Microfluid. Nanofluid.* **4**, 117–127 (2008).
[16] S. J. Woltman, G. D. Jay, and G. P. Crawford, *Nature Mat.* **6**, 929–938 (2007).
[17] A. d'Alessandro, B. Bellini, D. Donisi, R. Beccherelli, and R. Asquini, *IEEE J. Quantum Electr.*, **42**, 1084–1090 (2006).
[18] B. Bellini, A. d'Alessandro, and R. Beccherelli, *Opt. Mat.* **29**, 1019–1022 (2007).
[19] B. Bellini, J.-F. Larchanché, J.-P. Vilcot, D. Decoster, R. Beccherelli, and A. d'Alessandro *Applied Optics* **44**(33), 7181–7186 (2005).
[20] B. Bellini and R. Beccherelli "Modelling, design and analysis of liquid crystal waveguides in preferentially etched silicon grooves", *J. Phys. D: Appl. Phys.* **42**(4), 045111 (2009).
[21] F. Simoni and O. Francescangeli, *J. Phys.: Condens. Matter* **11**, R439–487 (1999).